Energy & Environmental Science

Accepted Manuscript

ROYAL SOCIETY OF CHEMISTRY

www.rsc.org/ees

Eldfellite, $NaFe(SO_4)_2$: An Intercalation Cathode Host for Low-Cost Na-ion Batteries

Preetam Singh, Konda Shiva, Hugo Celio, and John B. Goodenough*

Texas Materials Institute and Materials Science and Engineering Program
The University of Texas at Austin
Austin, TX 78712

*To whom correspondence should be addressed
E-mail: jgoodenough@mail.utexas.edu
Phone: 512-471-1646
Fax: 512-471-7612

Abstract

The mineral Eldfellite, $NaFe(SO_4)_2$, is characterized as a potential cathode for a Na-ion battery that is fabricated in charged state; its 3 V discharge versus sodium for reversible Na^+ intercalation is shown to have a better capacity, but lower insertion rate than Li^+ intercalation. The theoretical specific capacity for Na^+ insertion is 99 mAh g^{-1}. After 80 cycles at 0.1 C versus a Na anode, the specific capacity was 78 mAh g^{-1} with a coulomb efficiency approaching 100%.

Key Words: Rechargeable sodium battery; Na^+ intercalation; Fe^{3+}/Fe^{2+} redox energy.

Introduction

The need to liberate modern society from its dependence on the energy stored in fossil fuels has stimulated a world-wide effort to develop an economically competitive energy infrastructure based on the conversion of diffuse and variable wind and solar energy into electric energy that is stored in rechargeable batteries. Rechargeable batteries for this purpose fall into two classes: (1) stationary batteries that store electrical energy for the grid and (2) portable batteries that power electric vehicles (EVs). The success of the Li-ion battery to power the wireless revolution, an application that does not compete with fossil fuels, has already created a significant demand for lithium that may not be conveniently met if Li-ion rechargeable batteries under development are also to be used for both powering EVs and storing electrical energy for the grid.[1-4] Since sodium is abundant and widely available, there is increasing interest in the development of Na-ion batteries to complement the development of Li-ion batteries for storage of electrical energy. However, the larger size of the Na^+ ion makes it more difficult to identify insertion-compound hosts for reversible cathode reactions with Na^+ versus Li^+ as the working ion of a rechargeable battery.[5]

Considerable effort has been made to develop a cathode for a Na-ion battery and several potential cathodes have been identified such as $Na_2Ni_2TeO_6$[6] $Na_3V_2O_{2x}(PO_4)_2F_{3-2x}$,[7] Na_2FePO_4F,[8] $Na_2FeP_2O_7$,[9] $Na_4Fe_3(PO_4)_2(P_2O_7)$[10] and Nasicon structured $Na_2Fe_2(SO4)_3$[11], $Fe_2(SO_4)_3$[12] and $Na_2Fe(SO_4)_2.2H_2O$[13]. Although vacuum-dried $Na_2MnFe(CN)_6$ has been shown to provide fast reversible extraction of Na^+ at a voltage V = 3.4 V versus sodium with a long cycle life, the cyanide anion is toxic.[14-15] Therefore, there is an interest to identify other low-cost host cathodes for a Na-ion rechargeable battery. In this paper, we report the performance of reversible insertion of sodium and of lithium in $NaFe(SO_4)_2$. The host compound operates on the Fe^{3+}/Fe^{2+} redox couple on insertion of either Na^+ or Li^+ ions, and $Fe_2(SO_4)_3$ is known to give a V = 3.6 V versus lithium[16-17] corresponding to 3.3 V versus sodium.

Experimental

Since SO_4^{2-} polyanions decompose with the evolution of SO_2 at temperatures T > 600°C, a low-temperature synthesis was used to obtain $NaFe(SO_4)_2$, Eldfellite[18]. After dissolving 0.01 M of $NH_4Fe(SO_4)_2$ in 50 ml of water, 0.01 M of $NaHCO_3$ was added to the solution. Immediately, CO_2 gas comes out with the formation of the water-soluble $NaFe(SO_4)_2$. The water was

evaporated at 80°C, and the dry off-yellow powder product was transferred to an alumina crucible after grinding; the crucible was transferred to a tube furnace and heated at 200°C for 12 h and then at 350°C for 24 h. Alternatively, $NaFe(SO_4)_2$ was also synthesized from a mix of $Fe_2(SO_4)_2$ and Na_2SO_4; after heating, the resulting powder had an off-white color. The $NaFe(SO_4)_2$ synthesized by the solution route utilizing $NH_4Fe(SO_4)_2$ and $NaHCO_3$ was used in all the electrochemical and structural studies. The phase purity of the products were confirmed by powder X-ray diffraction (XRD) with a Philips X'Pert diffractometer and CuK_α radiation, λ= 1.514 Å, in Bragg-Brentano reflection geometry. A Rietveld structure refinement carried out with the Fullprof program verified the monoclinic $NaFe(SO_4)_2$ *(C12/m1)* structural model.

The microstructures of the product powders and pellets were examined with scanning electron microscopy (SEM) at an accelerating voltage of 2.0 kV (FEI Quanta 650 SEM). The composition and homogeneity of the compounds were confirmed by energy-dispersive X-ray (EDX) spectroscopy with a Bruker EDX system attached to the SEM instrument. An XPS study was also carried out to determine the oxidation state of the as-prepared material as well as at different states of electrochemical Na or Li insertion/extraction.

Electrochemical Characterization

For electrochemical measurements in a standard CR2032 coin cell, the composite cathode composition of 70:25:05 weight ratio $NaFe(SO_4)_2$, carbon black (Alfa Aesar), and polytetrafluoroethylne (PTFE, Kynarflex) was rolled into a thin sheet, punched into circular disks having a typical mass of 5-6 mg, and then dried in vacuum at 120°C for 12 h. Cell assembly was done at 25°C in a glovebox (MBraun) under Argon (H_2O < 0.1 ppm; O_2 < 0.1 ppm) with Whatman glass fiber as separator and, as electrolyte, 1 M $NaClO_4$ in 10% FEC in propylene carbonate (PC, Aldrich) for a Na-ion cell or 1 M $LiPF_6$ in 10% FEC in ethylene carbonate (EC, Aldrich) and diethylcarbonate (DEC, Aldrich) for a Li-ion cell. The galvanostatic cycling was performed in the voltage range 2.0 to 4.2 V versus both Li^+/Li and Na^+/Na. For *ex situ* X-ray photoelectron-spectroscopy (XPS) measurements, the coin cells were cycled to a requisite potential at a constant current density of 0.05 C. Following the battery cycling, the cells were disassembled inside an argon filled glovebox and the electrodes were washed several times with anhydrous dimethyl carbonate (DMC) to remove $NaClO_4$/$LiPF_6$ salt. The electrodes were dried and transferred into an ultrahigh-vacuum x-ray photoelectron-spectrometer chamber

without exposing them to air by employing a sample transfer interface. An XPS study was performed with a Kratos Axis Ultra, a multitechnique electron spectrometer (Manchester, U.K.). The monochromatic Al X-ray source (148.6 eV) was calibrated with the $3d_{5/2}$ line of silver; the XPS spectra were calibrated with reference to graphitic carbon at 284.5 eV in the electrode or adventitious carbon at 285 eV to check or correct the binding-energy of the peaks due to charging effects. Casa XPS analysis software was used for peak deconvolution, and line syntheses were conducted with a Gaussian-Lorentzian 70:30 curve fit and Shirley background subtraction of elemental spectra.

Results

The structure of $NaFe(SO_4)_2$ is shown in Fig. 1. The Na^+ and Fe^{3+} ions occupy octahedral sites in the *a – b* planes; these planes are bridged by (SO_4) polyanions that leave interplanar space for 2D Na^+ or Li^+ guest-ion diffusion.

The powder X-ray diffraction (XRD) pattern of as-prepared $NaFe(SO_4)_2$ is shown in Fig. 2(a); Fig. 2(b) shows the pattern for the composite electrode after 50 charge/discharge cycles. The Rietveld refinement of the as-prepared X-ray data is shown in Fig. 3. The observed pattern matches well that reported in JSPDS for $NaFe(SO_4)_2$ with space group *C12/m1*; the refinement had an R_{brag} = 3.5 %, R_f = 4.7%, R_p = 7.1%, R_{wp} = 8.9%, R_{exp} = 3.2% and χ^2 = 6.8%. The large difference between the calculated and observed XRD intensities which is also evident from the large values of the refinement parameters is not unusual for layered structures that commonly exhibit preferred orientations. The SEM images of the powder morphology, Fig. 4, reflect the planar layered structure; flakes of $NaFe(SO_4)_2$ are agglomerated into layer on layer of platelets. An EDX study, Fig. 4(c), confirmed the composition of the as-prepared material. The XPS study was carried out to investigate the electronic structure of the material to redox or electrochemical discharge processes. Since Fe (2p) spectra are accompanied by broad satellite peaks, the Fe (3p) spectra were also recorded; they generally appear as sharp characteristic peaks with low intensities. Fig. 5(a) and Fig. 5(c) show, respectively, the Fe (2p) and Fe (3p) spectra; they show the presence of iron mostly as Fe^{3+} before discharge in the as-prepared electrode material. Fig. 5(b) and Fig. 5(d), respectively, show the Fe (2p) and Fe (3p) spectra; the data clearly shows 90% of the iron in the Fe^{2+} state in the material discharged to 2V. The Fe (2p) and Fe (3p) peaks

observed in our study for the Fe^{2+} and Fe^{3+} state are consistent with the same core level peaks in iron sodium silicate glass.[19]

Electrochemical measurements were made with half-cells without further modification of the as-prepared $NaFe(SO_4)_2$. A circular-disk electrode of 5 to 6 mg containing 25% carbon and 5% PTFE was used. Figs. 6(a) and (b) show, respectively, cyclic voltammograms for Na and Li intercalation for the first 5 discharge/charge cycles over the voltage range $2.0 \leq V \leq 4.2\ V$ at a scan rate of 0.25 mV s^{-1}. The insertion rate of Li is seen to be faster than that of Na, particularly after the first cycle. The CV measures the surface redox voltage, which changes with the state of charge at the surface. Since the present material is an electronic insulator, insertion of Na is initially sluggish compared to the scan rate of the CV, so the state of charge changes more rapidly at the surface than in the bulk. The Li insertion is faster than the Na insertion; therefore, in the discharged cycles, the CV peaks are sharper and come together with fewer cycle as the mixed-valance on the iron atoms penetrates to the bulk. The CV for Li insertion also indicates another process occurs near 2V, which is manifest in the initial discharge as a capacity around 60 $mAhg^{-1}$(Fig. 7 (b)). Since the capacity is almost half of the theoretical capacity, this process is most likely a cation ordering transition. Although we expect stronger columbic interactions between the Na^+ ions than between the Li^+ ions, the slower rate of insertion of Na means a more heterogeneous Na distribution, which would suppress long range mobile cation ordering.

Figures 7(a) and (b) show, respectively, the voltage profiles for Na and Li discharge/charge at 0.05C for the first cycle followed by 0.2C for subsequent cycles. Surprisingly, the capacity is larger for Na than for Li intercalation in these experiments. The data show single-phase, reversible insertion reactions with both Na and Li anodes. The theoretical capacity for reversible intercalation of one Na per $NaFe(SO_4)_2$ molecule is 99 mAh g^{-1}. After 80 cycles, a capacity for Na insertion at 0.1 C was 78 mAh g^{-1} with a coulomb efficiency approaching 100%, Fig. 8. However, Figs 7(c) and 8 show a sharp capacity decrease with increasing rate greater than 0.1 C; but this capacity loss is recovered on decreasing the rate back from 2 C to 0.1C, Fig. 8. The material shows robust reversible capacity with various rate of charge and discharge and the intercalation process seems to be single phase. In order to confirm that a single-phase intercalation occurs during charge-discharge, we have done the *ex-situ* XRD studies, which are included in Fig. 9. After discharge on sodium intercalation, we observed a shift to the lower angle of all the XRD peaks compared to the parent material, and after recharge

of the discharged material, all the XRD peaks shifted to their original position. A Na half-cell is used to test the Na intercalation process and charge-discharge cycling rates. The $NaFe(SO_4)_2$ cathode presented here exists in the charged state. Since the cathode would be used in a rechargeable battery, one can start with either a charged or discharged.

Conclusions

The mineral Eldfellite, $NaFe(SO_4)_2$, was synthesized by a low-temperature process and evaluated as a potential cathode for a Na-ion battery. It offers a low-cost rechargeable Na-ion electrode with a discharge voltage $V \approx 3.0$ V versus sodium at a 0.1C rate with a capacity near 80 mAh g^{-1} for a relatively long life. A Na half-cell is used to test the Na intercalation process. Since the cathode would be used in rechargeable battery, one can start with either a charged or discharged cathode.

Acknowledgements

This work was supported by the Robert A. Welch Foundation (Grant F-1066).

References

1. K. Mizushima, P. C. Jones, P. J. Wiseman, & J. B. Goodenough, Li_xCoO_2 (0<x<1): A new cathode material for batteries of high energy density. Mater. Res. Bull. 15, 783–789 (1980).
2. M. M. Thackeray, W. I. F. David, P. G. Bruce, & J. B. Goodenough, Lithium insertion into manganese spinels. Mater. Res. Bull. 18, 461–472 (1983).
3. A. K., Padhi, K. S. Nanjundaswamy, & J. B. Goodenough, Phospho-olivines as positive-electrode materials for rechargeable lithium batteries. J. Electrochem. Soc. 144, 1188–1194 (1997).
4. J. M. Tarascon, Is lithium the new gold? Nat. Chem. 2, 510 (2010).
5. C. Delmas, J. J. Braconnier, C. Fouassier, & P. Hagenmuller, Electrochemical insertion of sodium in Na_xCoO_2 bronzes. Solid State Ion 3–4, 165–169 (1981).
6. A. Gupta, C. Buddie Mullins, J. B. Goodenough, $Na_2Ni_2TeO_6$: Evaluation as a cathode for sodium battery, Journal of Power Sources, 243, (2013)817–821.
7. P. Serras, V. Palomares, A. Goñi, I. Gil de-Muro, P. Kubiak, L. Lezama and T. Rojo, High voltage cathode materials for Na-ion batteries of general formula $Na_3V_2O_{2x}(PO_4)_2F_{3-2x}$, *J. Mater. Chem.*, 2012,22, 22301-22308
8. B. L. Ellis, W. R. M. Makahnouk, Y. Makimura,, K. Toghill, & L. F. Nazar, A multifunctional 3.5V iron-based phosphate cathode for rechargeable batteries. Nat. Mater. 6, 749–753 (2007).
9. P. Barpanda, et al. Sodium iron pyrophosphate: A novel 3.0V iron-based cathode for sodium-ion batteries. Electrochem. Commun. 24, 116–119 (2012).
10. H. Kim, et al. New iron-based mixed-polyanion cathodes for lithium and sodium rechargeable batteries: combined first principles calculations and experimental study. J. Am. Chem. Soc. 134, 10369–10372 (2012).
11. P. Barpanda, G. Oyama, S. Nishimura, S. Chung, A. Yamada , A 3.8-V earth-abundant sodium battery electrode, Nature Commun. 5, 4358, doi:10.1038/ncomms5358 (2014).

12. C. W. Mason, I. Gocheva, H. E. Hoster and D. Y. W. Yu, Iron(III) sulfate: a stable, cost effective electrode material for sodium ion batteries, Chem. Comm., 50, 2249-2251 (2014).
13. Y Meng, S. Zhang and C. Deng, Superior sodium–lithium intercalation and depressed moisture sensitivity of a hierarchical sandwich-type nanostructure for a graphene–sulfate composite: a case study on $Na_2Fe(SO)_2.2H_2O$, J. Mater. Chem. A, 3, 4484-4492 (2015).
14. Prussian blue: a new framework of electrode materials for sodium batteries , Y. Lu, L. Wang, J. Cheng and J. B. Goodenough, ***Chem. Comm.***, **48**, 6544-6546 (2012).
15. Removal of Interstitial H_2O in Hexacyanometallates for a Superior Cathode of a Sodium-Ion Battery, J. Song , L. Wang, Y. Lu, J. Liu, B. Guo, P. Xiao, J. Lee, X. Yang, G. Henkelman, and J. B. Goodenough, *J. Am. Chem. Soc.*, 2015, 137 (7), 2658–2664.
16. Padhi, A. K., Nanjundaswamy, K. S., Masquelier, C. & Goodenough, J. B. Mapping of transition metal redox energies in phosphates with NASICON structure by lithium intercalation. J. Electrochem. Soc. 144, 2581–2586 (1997).
17. Manthiram, A. & Goodenough, J. B. Lithium insertion into $Fe_2(SO_4)_3$ frameworks. J. Power Sources. 26, 403–408 (1989).
18. T. Balić-Žunić, A. Garavelli, P. Acquafredda, E. Leonardsen, and S. P. Jakobsson Eldfellite, $NaFe(SO_4)_2$, a new fumarolic mineral from Eldfell volcano, Iceland Mineralogical Magazine, 73, 51-57(2009*).*
19. A. Mekki, D. Holland, C. F. McConville, M. Salim, An XPS study of iron sodium silicate glass surfaces, J. Non-Crystalline Solids, 208, 267–276 (1996).

Figure Captions

Figure 1. Crystal structure of Eldfellite, $NaFe(SO_4)_2$ (a) planner view and (b) vertical stacking.

Figure 2. XRD patterns of (a) as prepared $NaFe(SO_4)_2$ and (b) composite cathode after 50 cycle of charge/discharge vs Na electrode.

Figure 3. Rietveld refined Power XRD profile of as prepared $NaFe(SO_4)_2$.

Figure 4(a), (b) SEM images and (c) EDX profile of as prepared $NaFe(SO_4)_2$.

Figure 5. Fe(2p) XPS spectra of (a) as prepared $NaFe(SO_4)_2$ and (b) after discharge up to 2V *vs* Na electrode and Fe(3p) core level spectra of (c) as prepared $NaFe(SO_4)_2$ and (d) after discharge up to 2V *vs* Na electrode

Figure 6. Cyclic voltammograms for the 1^{st} to 5^{th} cycle for (a) $NaFe(SO_4)_2$ – Na and (b) $NaFe(SO_4)_2$ – Li.

Figure 7. Galvanostatic charge-discharge profiles at 0.05 C, subsequent cycles at 0.2 C rate for (a) $NaFe(SO_4)_2$ *vs* Na electrode and (b) $NaFe(SO_4)_2$ *vs* Li electrodes, (c) $NaFe(SO_4)_2$ *vs* Na at different C rates.

Figure 8. $NaFe(SO_4)_2$ *vs* Na (a) coulomb efficiency at 0.2 C and (b) capacity at different C rates.

Figure 9. powder xrd pattern of (a) $NaFe(SO_4)_2$ electrode before cycling, (b) After discharge up to 2.0V and (c) after recharging up to 4.0V.

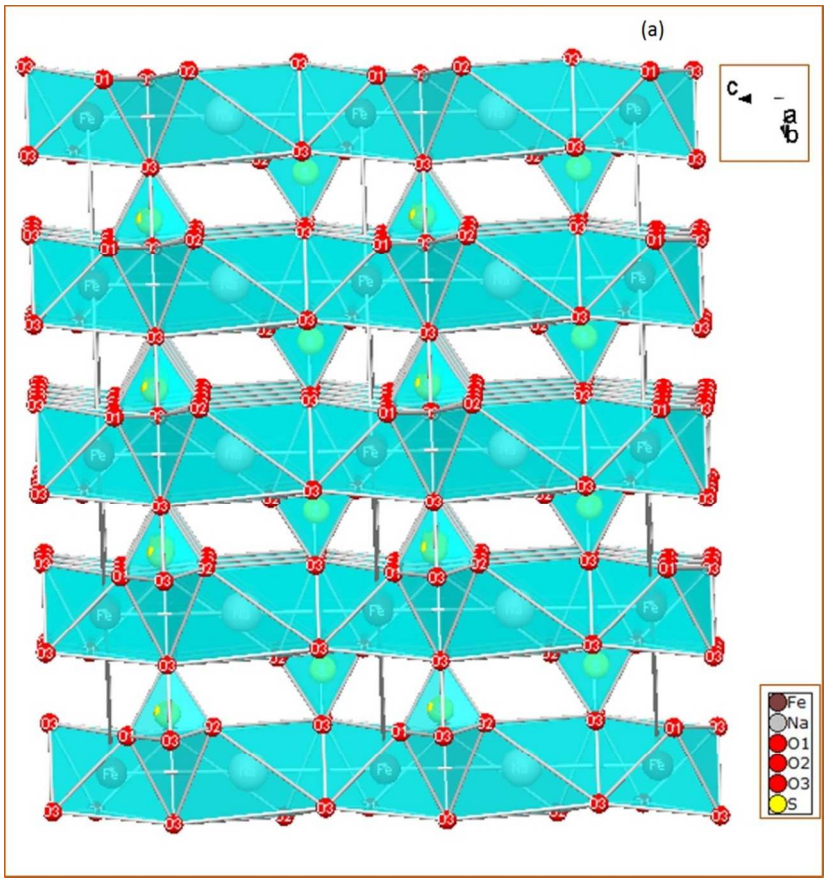

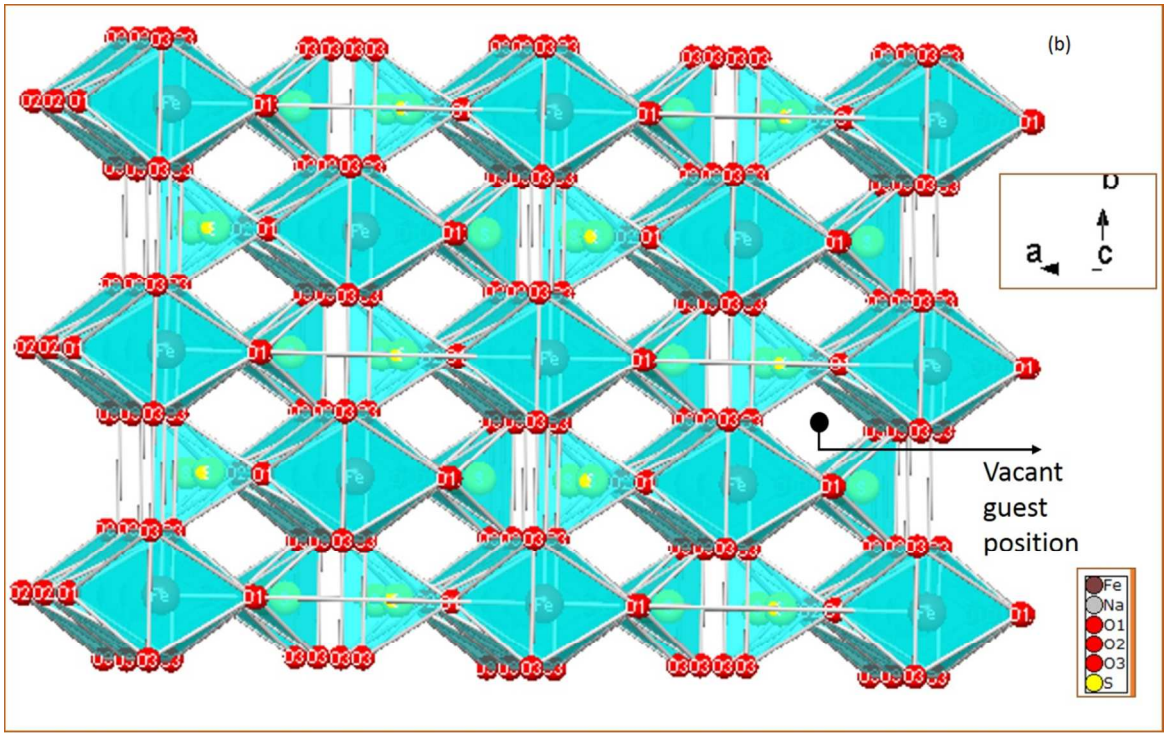

Figure 1.

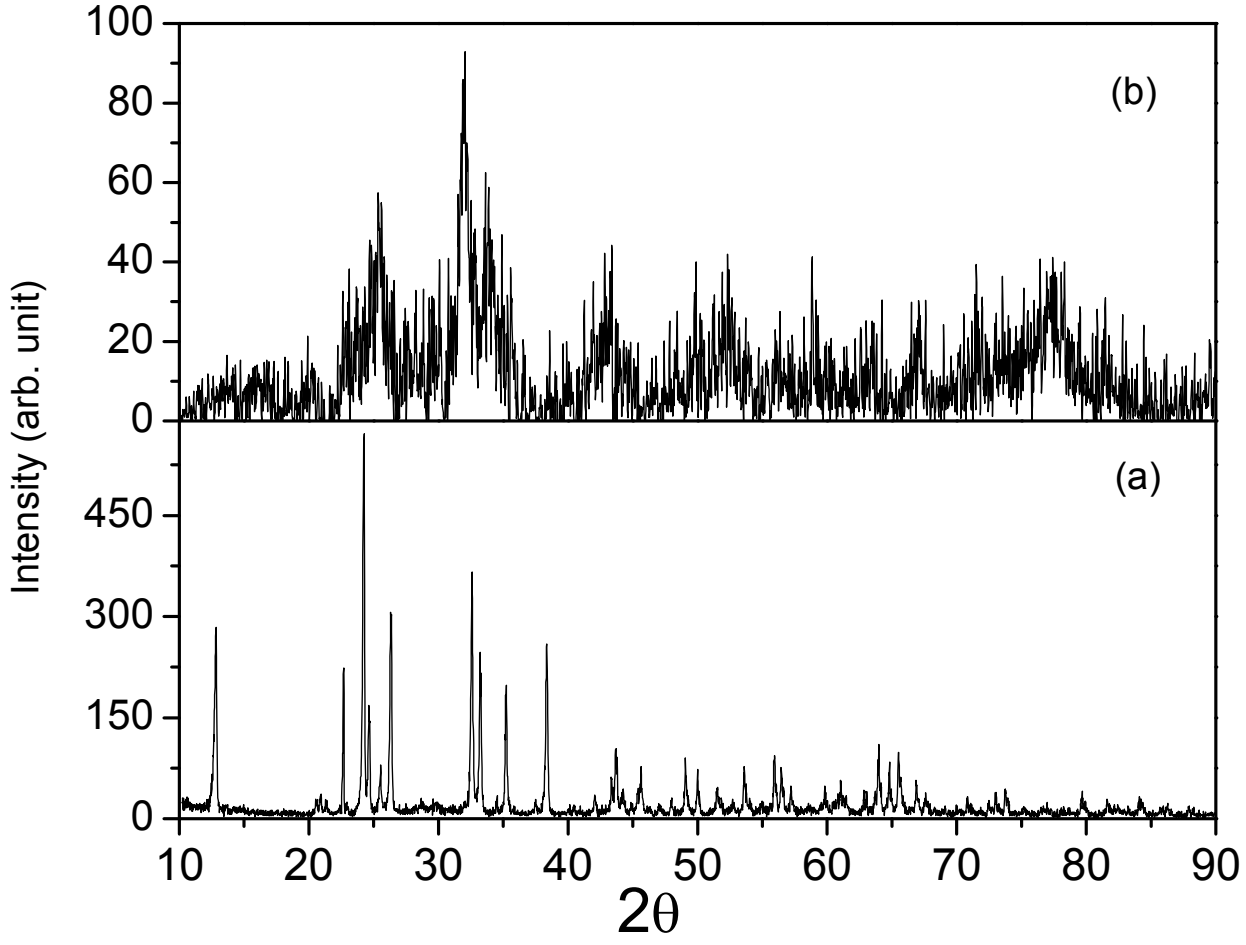

Figure 2.

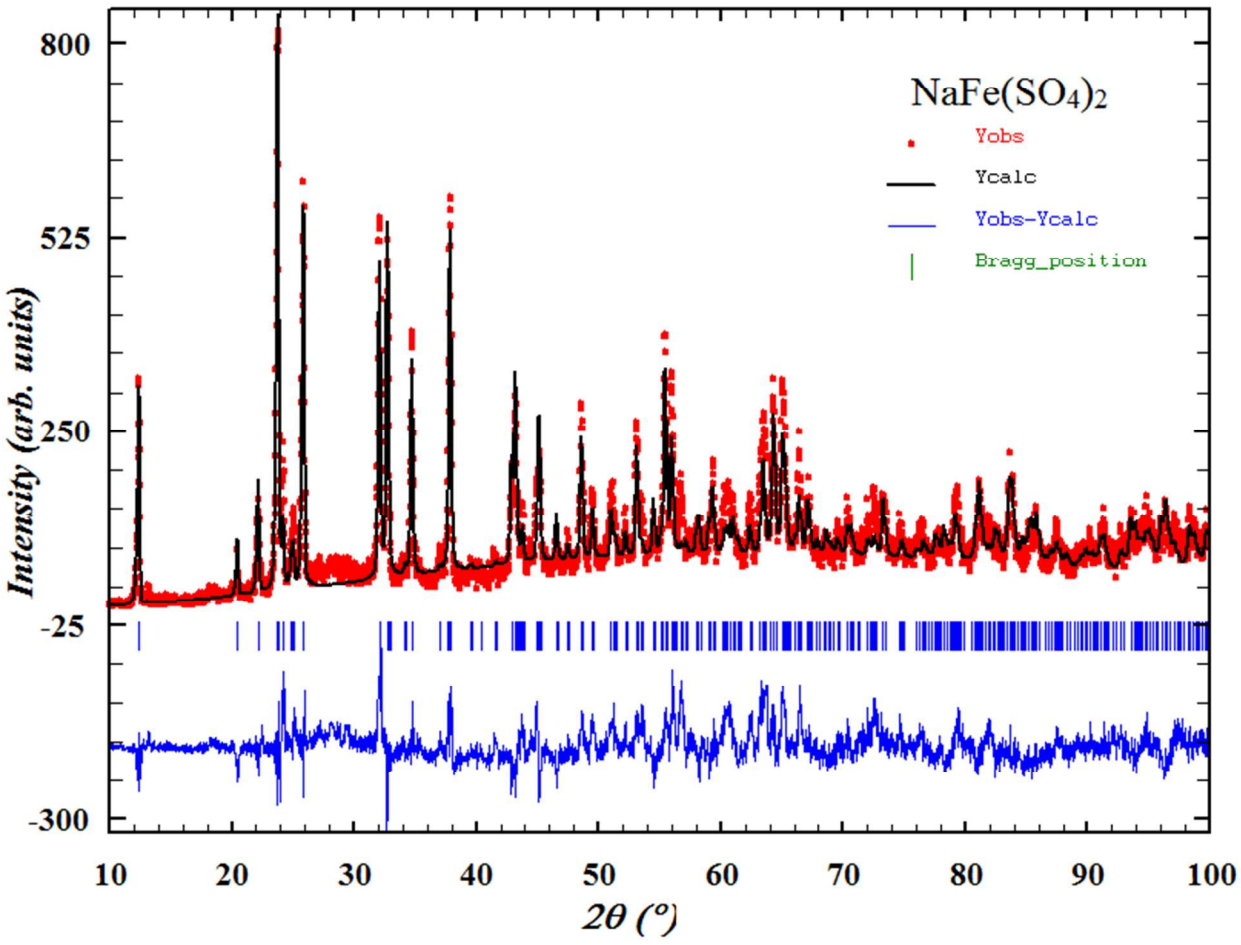

Figure 3.

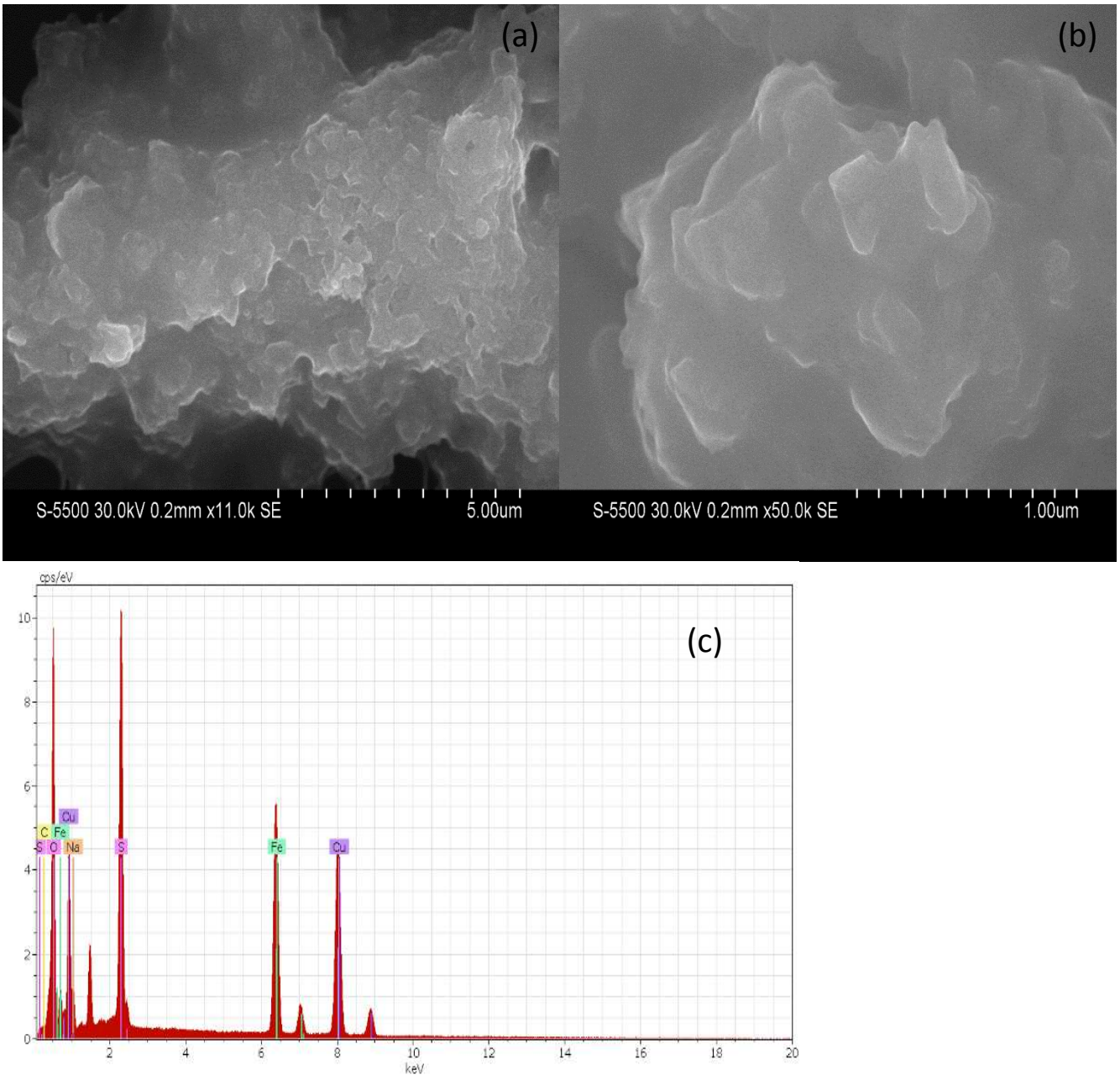

Figure 4.

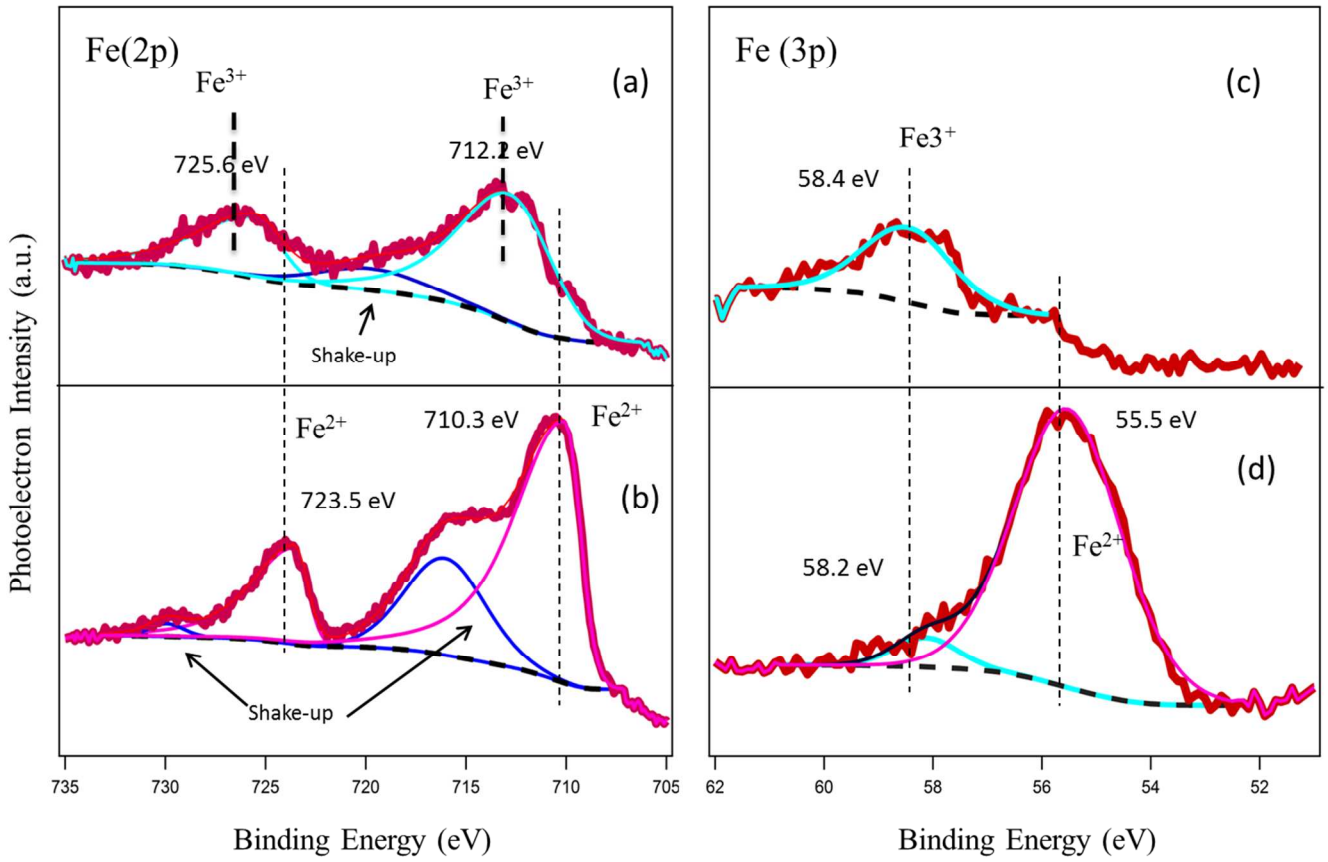

Fig. 5.

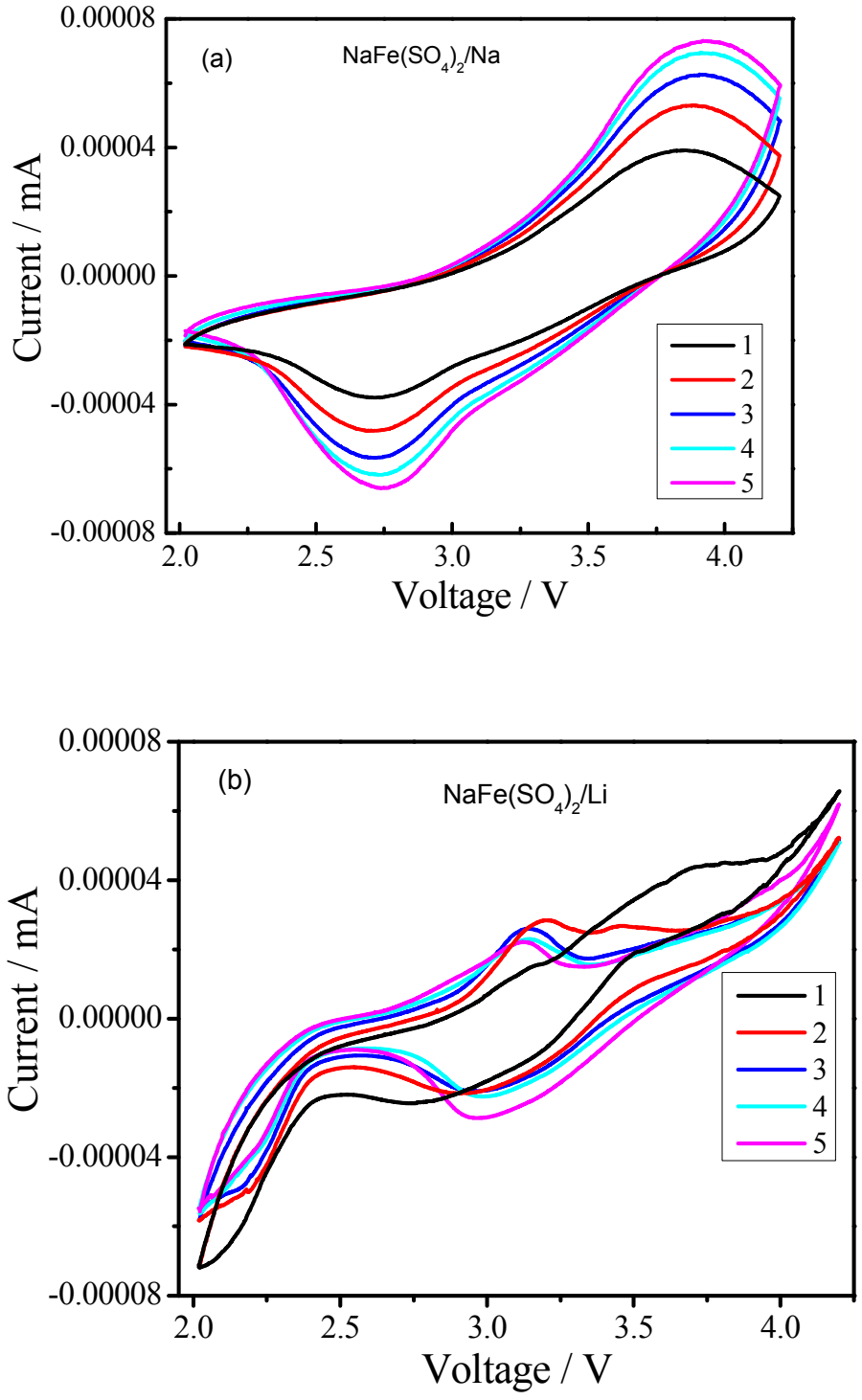

Figure 6.

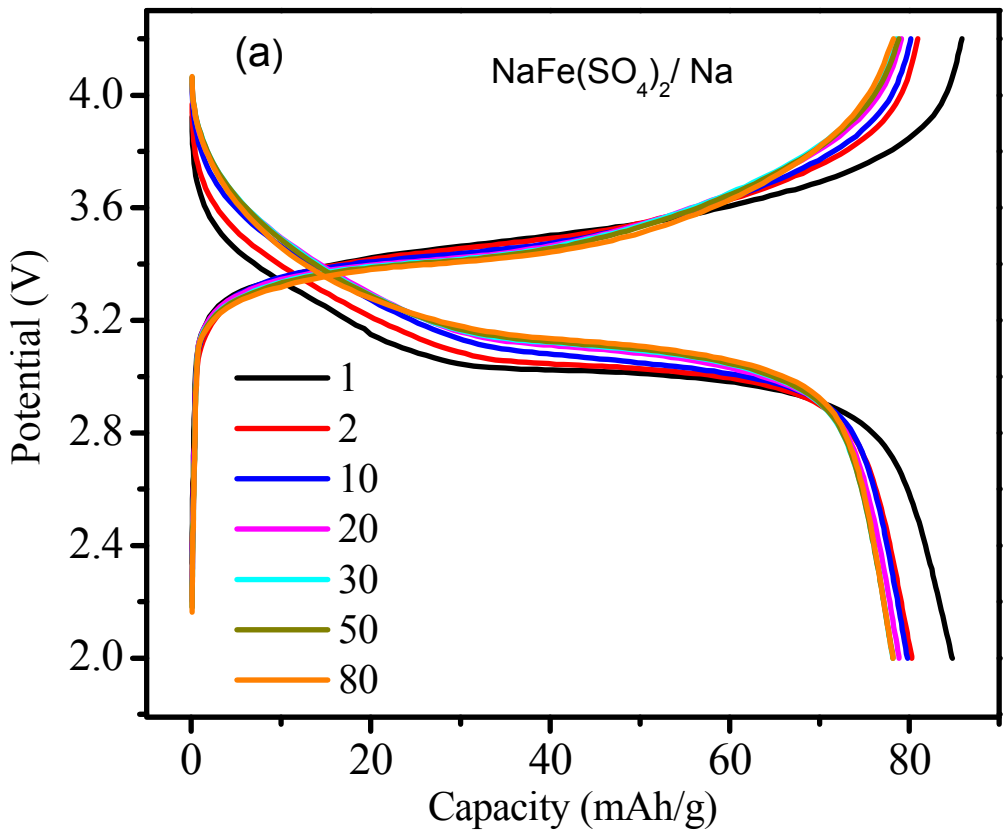

Figure 7(a)

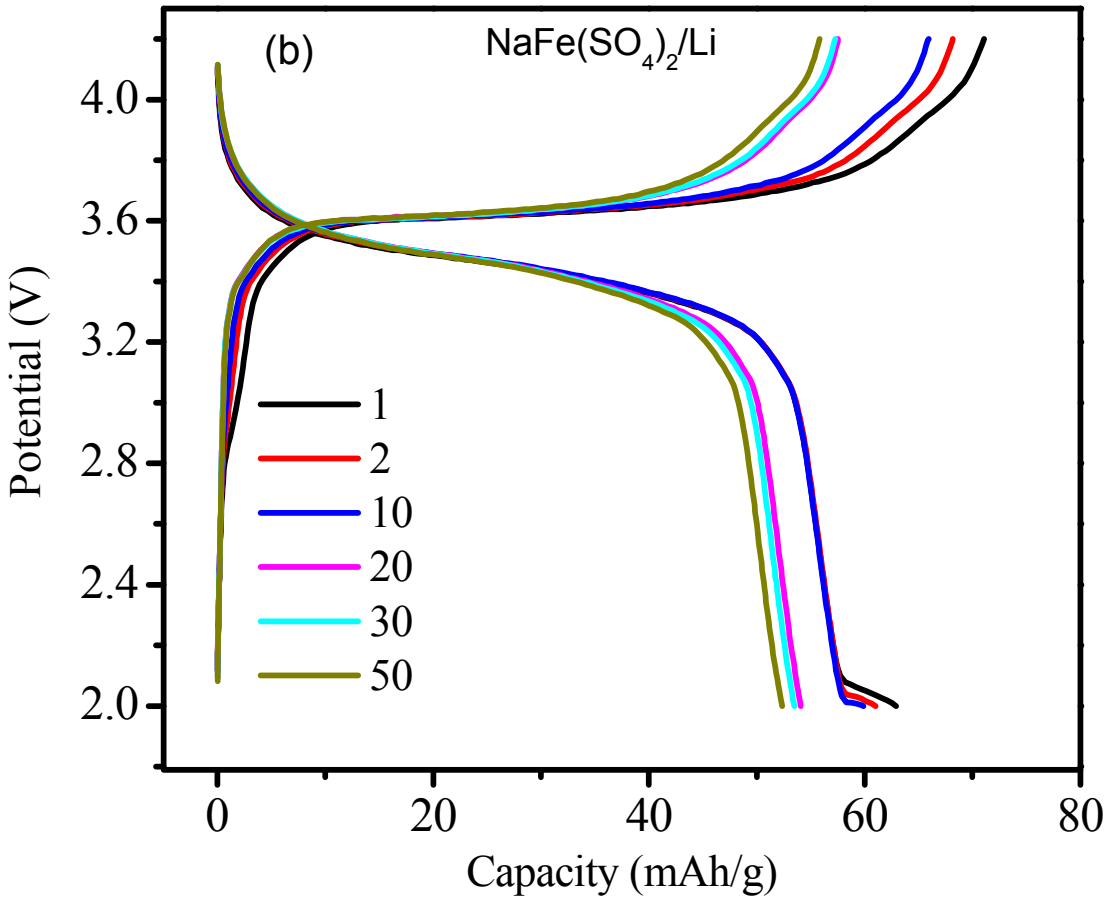

Figure 7 (b).

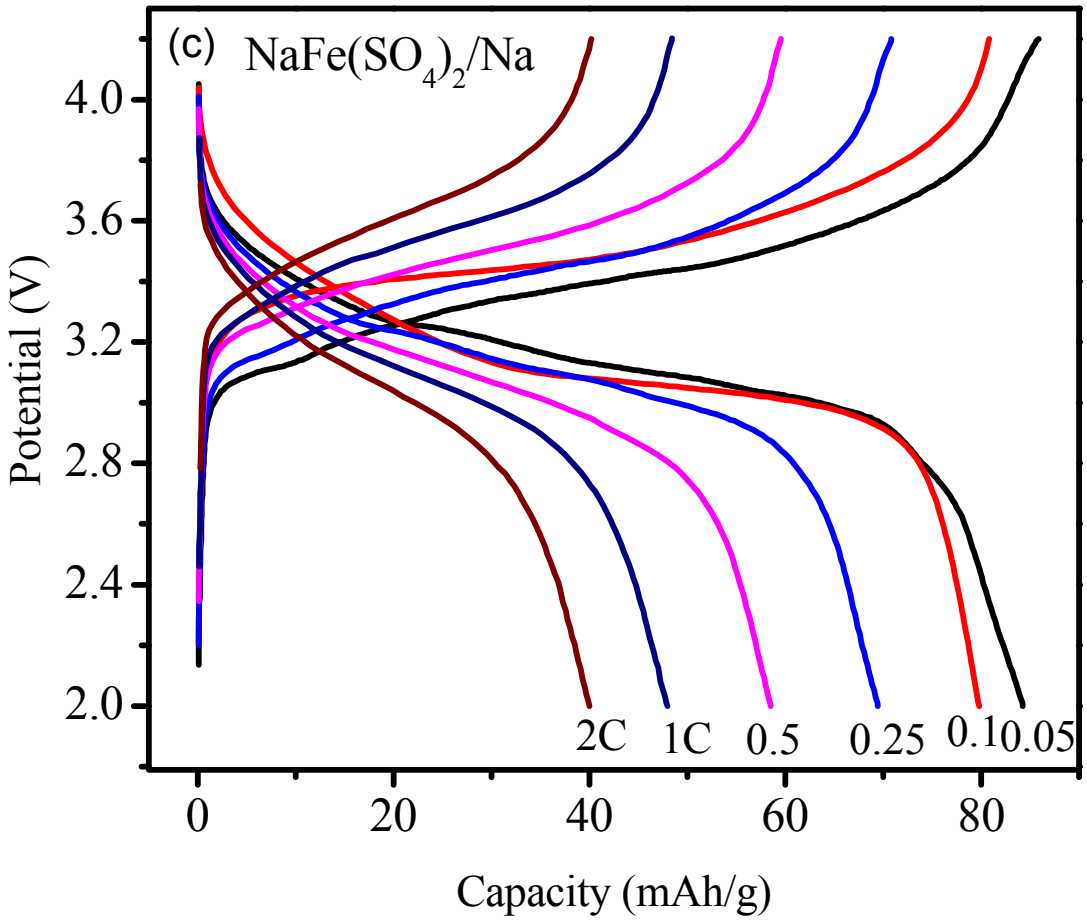

Figure 7(c).

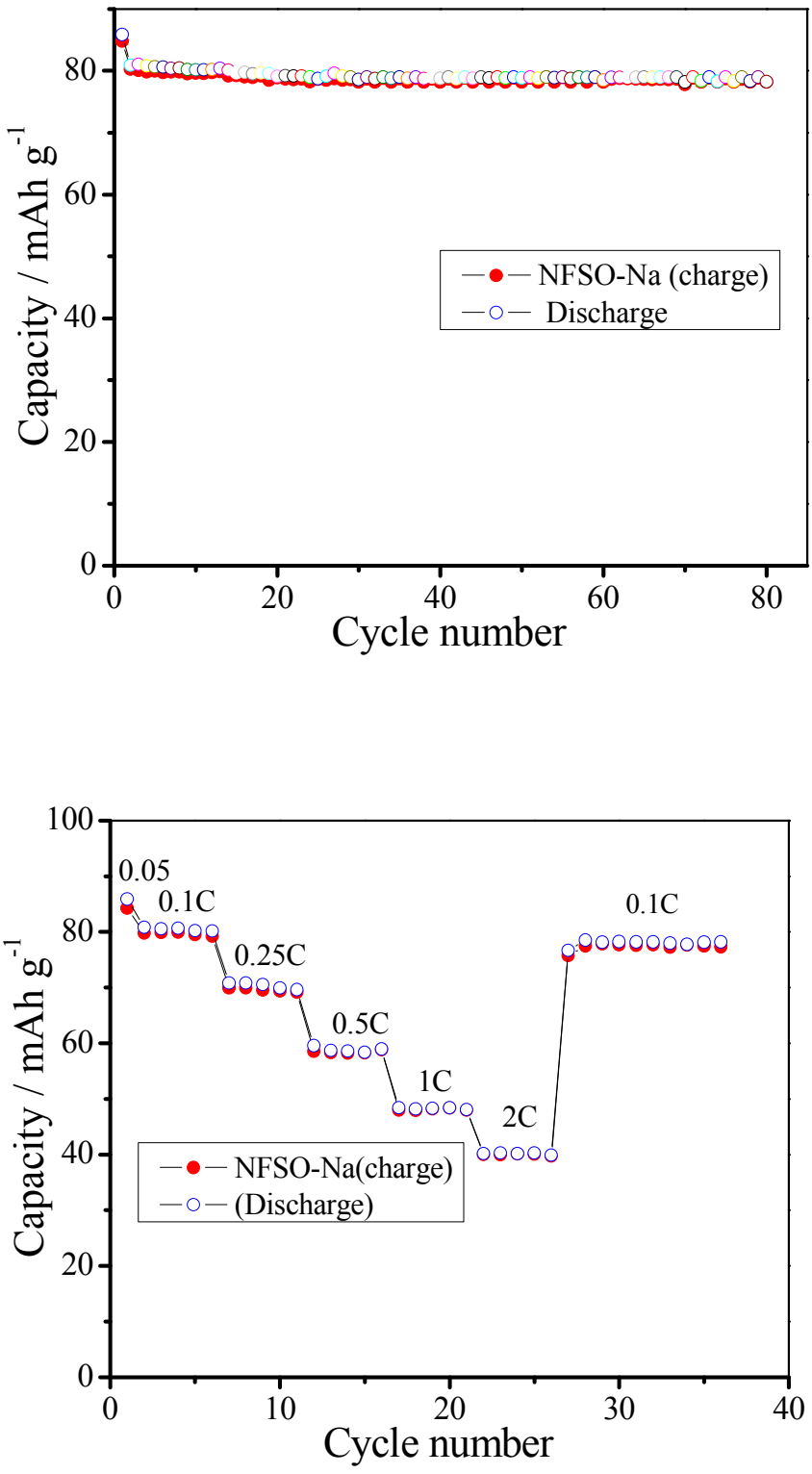

Figure 8.

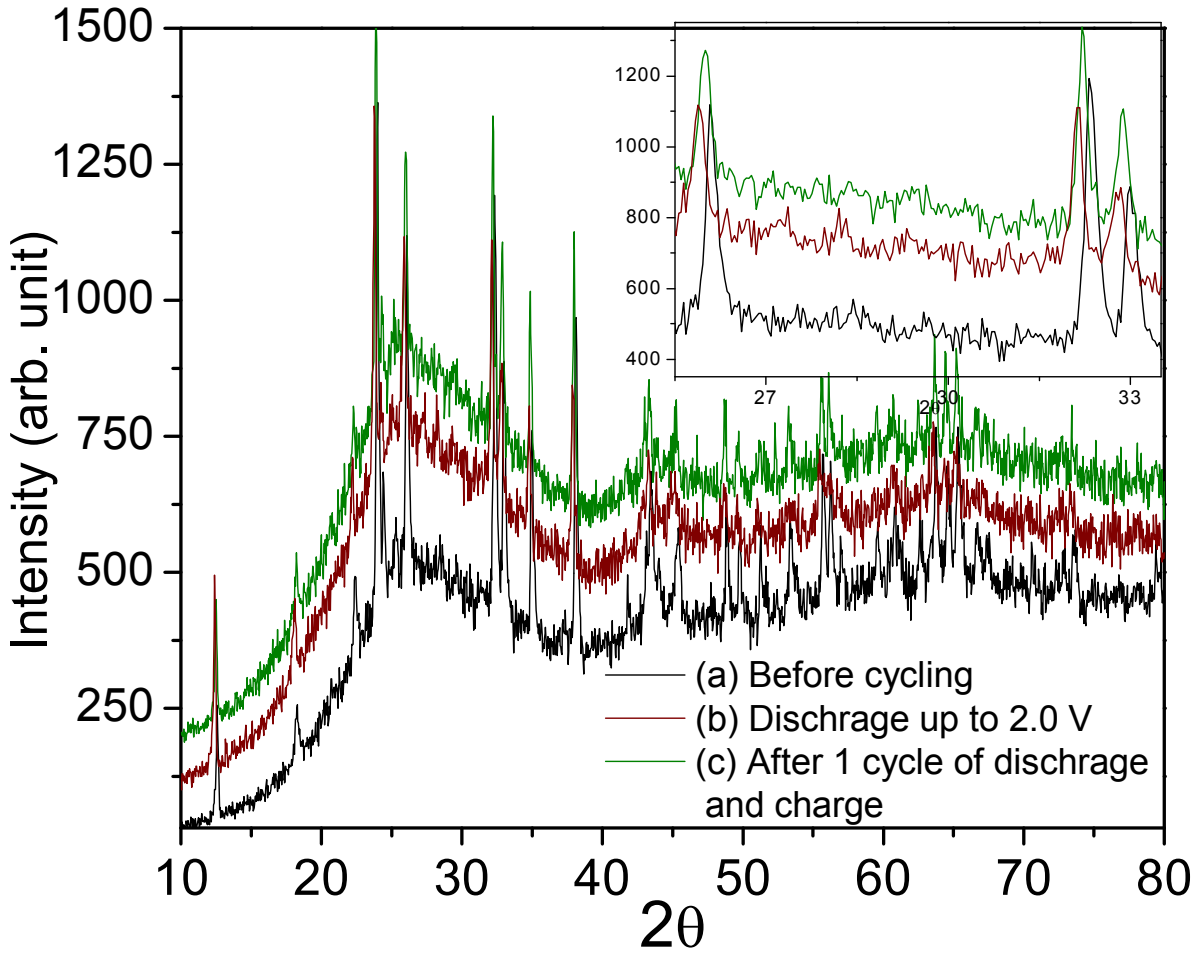

Fig.9

Table of Content:

The mineral Eldfellite, $NaFe(SO_4)_2$, is characterized as a potential cathode for a Na-ion battery that can be fabricated in charged-state.